ESO-74-F
July 1998

Fermilab Library
0 1160 0067557 3

VLT Unit Telescope, suitability for interferometry: first results from acceptance tests on subsystems

B. Koehler

European Southern Observatory (ESO), Karl-Schwarzschild Str. 2, D-85748 Garching, Germany

ABSTRACT

The Very Large Telescope (VLT) project includes an interferometric mode which consists in combining coherently the four 8-m telescopes as well as a number of 1.8-m Auxiliary Telescopes to achieve milli-arcsecond angular resolution. This mode, referred to as the VLT Interferometer (VLTI), imposes specific requirements on the whole observatory and, in particular, on the telescopes. One of these specific requirements is the very high stability required on the Optical Path Length (OPL) at the level of a few tens of nanometers. To verify the feasibility of achieving this requirement, a number of studies have been performed in the past years with encouraging results. In the last months, the readiness of major VLT sub-systems permitted to start the verification of these conclusions by test. This paper presents these first results on OPL stability obtained during acceptance testing on several subsystems of the VLT 8-m Unit Telescopes.

Keywords: Interferometry, Very Large Telescope, VLTI , Performance, Visibility loss, Vibrations

ESO-74-F

1. INTRODUCTION

One of the specificity and most exciting features of the VLT resides in its interferometric capability which is an integral part of the project since its beginning. In this mode called the VLT Interferometer (VLTI)[1], the four 8-m Unit Telescopes (UT) as well as a number of 1.8-m Auxiliary Telescopes (AT) are combined coherently to form interference fringes. The particularity of this mode is to provide a very high angular resolution (up to 0.6 milli-arcsecond when using the largest 200-m baseline between AT's in the visible) combined with a very high sensitivity (when using the 50m² collecting area of each UT).

The interferometric mode sets a number of stringent requirements on the whole observatory and, in particular, on the telescopes themselves. Among them is the very high stability required on the Optical Path Length (OPL) at the level of a few tens of nanometers. This is necessary to avoid significant smearing of the fringes which would spoil the accuracy on the measurement of the fringe contrast; the prime observable of a stellar interferometer. This represents a real challenge when considering the size, mass and complexity of an 8-meter class telescope exposed to its environment (wind, seismic, etc.).

In order to tackle this issue, a sound system engineering approach is necessary. This approach is illustrated in Figure 1. It starts with the definition of error budgets[2] which allocate values for the various error sources. From these, sub-system requirements are defined and first verification by studies are performed to validate or update the error budget and/or the sub-system requirements. This step has been reported in previous papers[3,4,5]. The present paper reports on first results obtained during the next validation step for the UT, namely verification by test on the hardware at sub-system level. The next performance validation for the fully integrated UT will occur during commissioning of UT#1 later this year, after first light.

The fringe contrast loss allocated for vibrations inside each telescope results from the following criteria: the contrast loss due to instrumental OPL fluctuation shall remain smaller (one half) of that created by the atmosphere. This means a contrast loss of 5% over the atmospheric coherence time at the observing wavelength. This loss shall then be distributed over each telescope, each delay line and the other optics in each interferometer arm. This leads to a loss of less than 1% for each telescope which translates, as a function of the observing wavelength, into the OPL fluctuations defined in Table 1.

Observing wavelength (μm)	0.6 Visible	2.2 near IR	10 Thermal IR
Detector exposure time (msec)	10	48	290
Requirement on OPL stability (nanometers rms)	***14***	***50***	***225***

Table 1: **Requirements on OPL stability due to vibrations inside each telescope**

SEP 17 1998

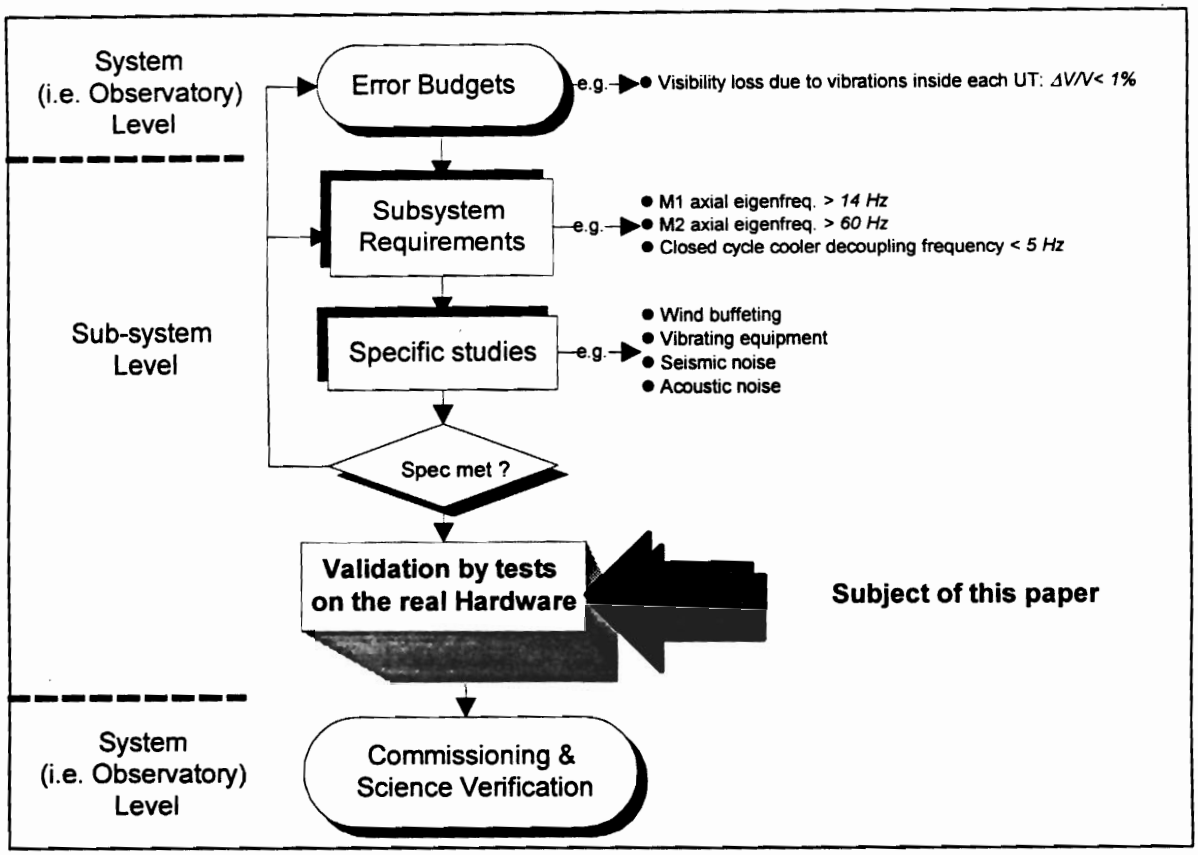

Figure 1: System engineering process for performance assessment and verification.

2. ENCLOSURE VIBRATIONS

The purpose of the tests performed in July 1997 during acceptance testing of the first enclosure was to verify the level of vibration generated by the enclosure during operation. The enclosure is a heavy piece of equipment which rotates (for slewing and for tracking), which is exposed to wind shaking, and which includes a number of mechanisms potentially generating vibrations. By design, the enclosure building is de-coupled from the telescope pier but vibration can nevertheless be transmitted through the ground. The following disturbances were included in the test objectives:

- Dome rotation during:
  - tracking,
  - slewing
- Small mechanisms (see Figure 2)
  - windscreens,
  - louvers,
  - ventilation doors,
- Wind shaking

The latter disturbance could unfortunately not be measured due to exceptionally low wind speeds during the measurement campaign. Previous studies have shown, however, that this disturbance shall not be significant owing to its low frequency characteristic. We plan to verify this conclusion during the commissioning test on UT#1 foreseen later this year.

At the time of these measurements, the telescope was not fully integrated, preventing a direct vibration measurement on the telescope structure. The principle was therefore to measure the ground acceleration at the bottom of the telescope pier during operation of the enclosure and to feed the resulting acceleration to the detailed FE Model of the telescope used previously during the study phase[5]. The OPL fluctuation at the Coudé focus was then computed from the displacement of all mirrors

(M1 to M8). Acceleration was also measured in the delay line tunnel and on the lower part of the partially integrated telescope structure, for indication only.

The test setup is shown on Figure 3, Figure 4 and Figure 5. It includes the following hardware:

- 4 low-noise Wilcoxon Accelerometers 731A
- 2 Sunstrand QA2000 accelerometers
- 2 Kinemetrics SS1 seismometers
- 2 DSPT SigLab acquisition units + PC running Matlab

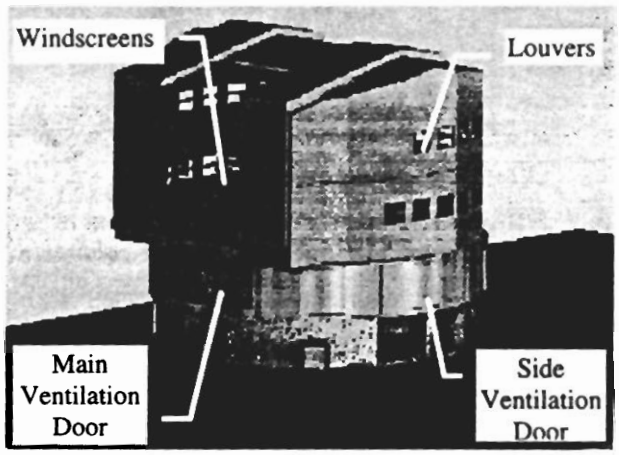

Figure 2: The VLT Enclosure mechanisms

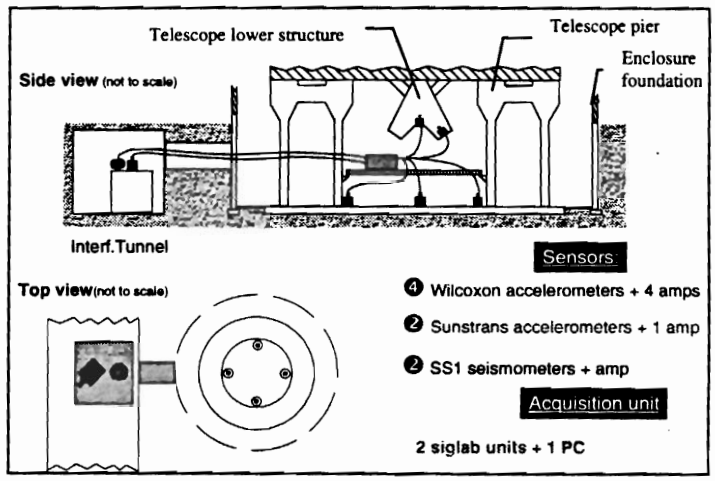

Figure 3: Measurement setup for the Enclosure vibrations. Acceleration of the ground is measured at the bottom of the telescope pier and is later fed through a FE model of the Telescope.

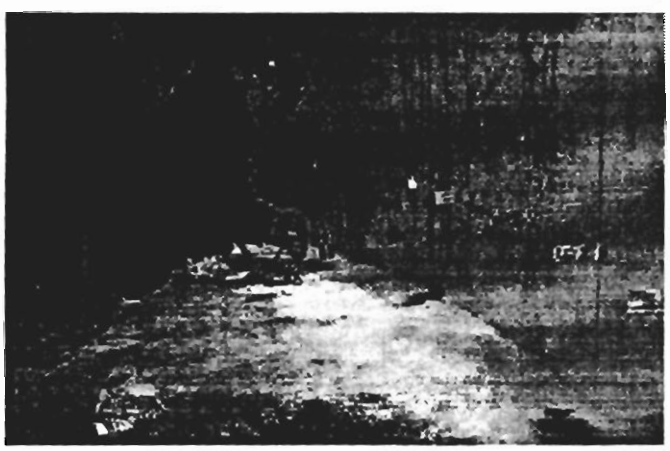

Figure 4: One of the four Wilcoxon accelerometers 731A monitoring the vertical ground motion at the bottom of the telescope pier.

Figure 5: The acquisition chain with accelerometer amplifiers and 2 SigLab digital acquisition units connected to a PC running Matlab.

Figure 6 provides an example of the ground acceleration measured during operation of the louvers. Even though these mechanisms involve relatively small moving masses, their effect at the bottom of the telescope pier is clearly visible owing to the extremely high sensitivity of the accelerometers. Figure 7 provides an other example of intermediate results showing the Power Spectral Density (PSD) of the vertical ground motion at the bottom of the telescope pier when the enclosure is rotating at different tracking speeds.

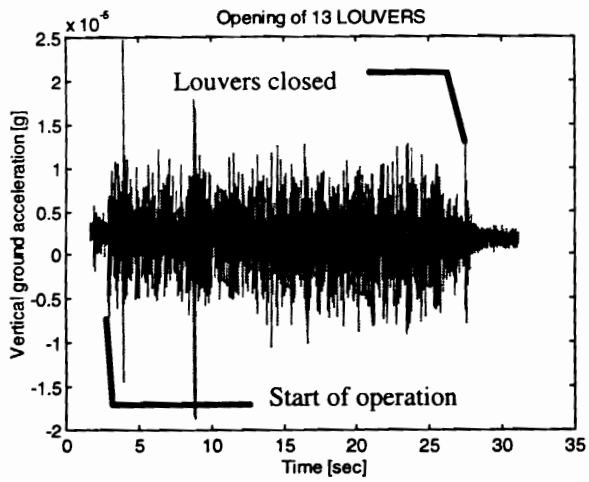

Figure 6: Example of ground acceleration due to operation of enclosure mechanisms: opening 13 louvers simultaneously.

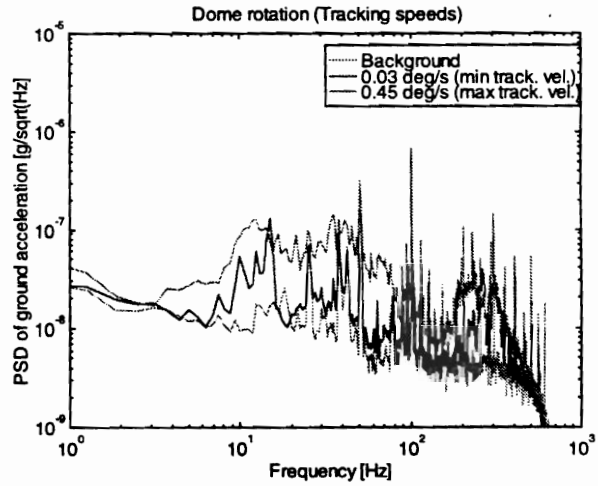

Figure 7: PSD of the vertical ground acceleration at the bottom of the telescope pier during enclosure rotation at tracking speeds.

Figure 8 and Figure 9 summarize the results obtained in terms of fringe contrast loss inside the UT for the various disturbances and at three observing wavelengths: Visible (0.6 μm), near IR (2.2μm), and thermal IR(10μm).
At the time of these measurements, the electrical power for the Telescope Area, and in particular for the enclosure, was supplied by two temporary diesel generators running at 1500 rpm. The associated disturbance can be seen on Figure 7 (the 25Hz line and its harmonics) as well as on Figure 8 when comparing the visibility loss with that obtained when the generators were switched off (last case of Figure 8). This disturbance was however sufficiently low not to disturb the rest of the campaign. As can be seen from Figure 8, the effect of operating the mechanisms is negligible for the infrared wavelengths. It remains below or very close to the specification for visible wavelengths. Together with the fact that these mechanisms will be operated only occasionally, it indicates that they will not disturb significantly interferometric observations. The last two cases of Figure 8 show that the disturbance created by somebody walking in the enclosure basement can clearly be seen but remains acceptable.

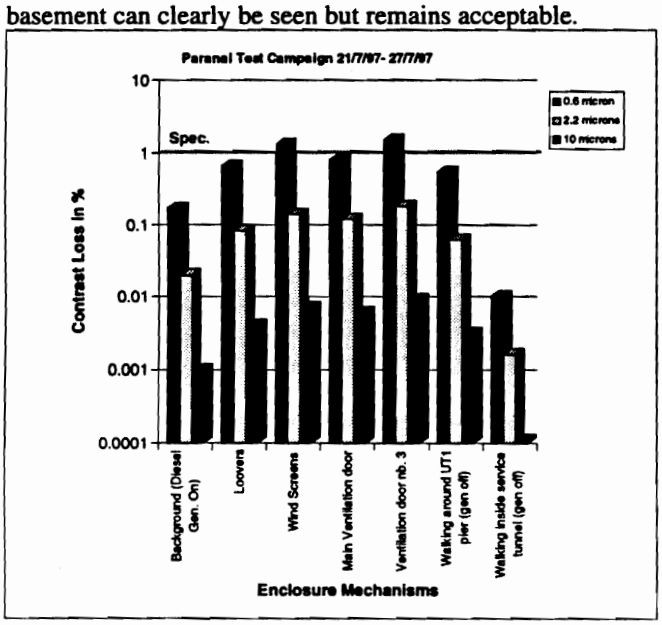

Figure 8: Summary of contrast loss due to vibration inside the UT when operating the enclosure mechanisms.

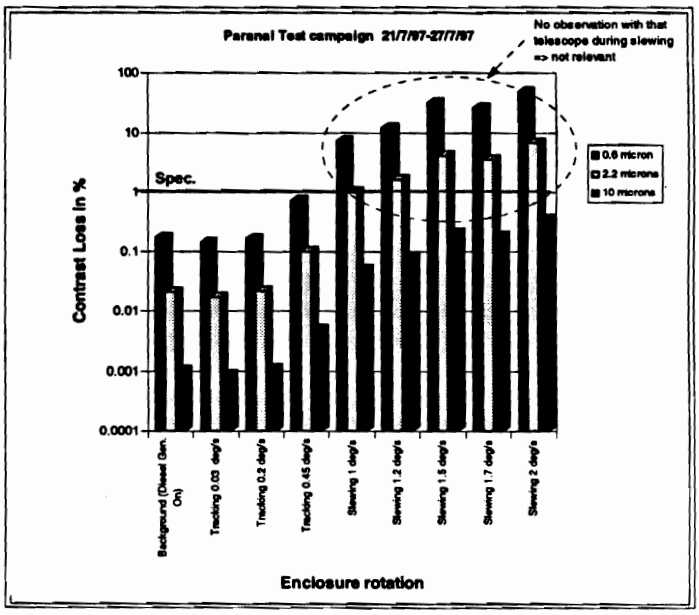

Figure 9: Summary of contrast loss due to vibration inside the UT when rotating the enclosure.

Excellent results were obtained concerning the impact of enclosure rotation at all tracking speeds, as seen on Figure 9. To limit technical risk, the design of the telescope/enclosure control system has foreseen the possibility to move the enclosure in step mode where the enclosure would be rotated only when beam obstruction is about to occur and in co-ordination with the interferometric instrument. The present results show that this more complicated mode will probably not be required.

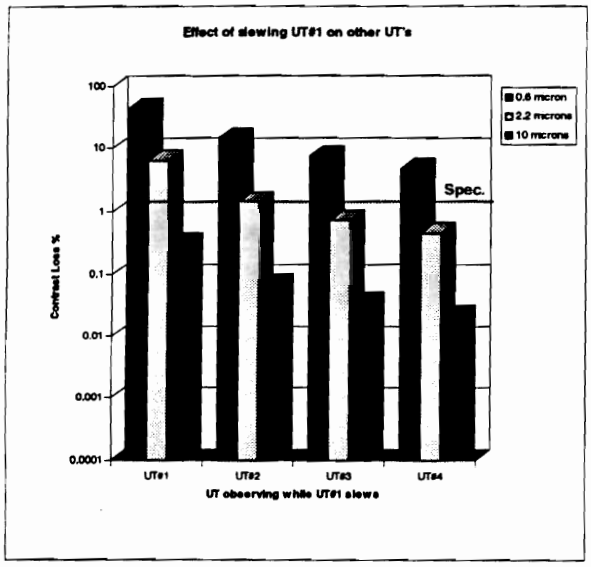

Figure 10: Simulated impact on other UT's when slewing the enclosure of UT#1 at 2 deg/sec. It is based on modeling the propagation of vibration in the ground using the Paranal ground transfer function characteristics.

As far as disturbance during slewing of the enclosure is concerned, Figure 9 shows that the impact on the fringe contrast would be excessively high if the telescope was observing when its enclosure is slewing. This case is, of course, not directly relevant. The relevant cases are the impact on other telescopes UT or AT assuming that one telescope, used for standalone observation, is slewing while the others are used for interferometric observations. These cases could not be measured during that campaign for practical reasons (Enclosure #2 and UT#2 were only at a very early stage of integration). It is planned to address this case during the commissioning tests, next summer by rotating Enclosure#2 and monitoring vibrations on UT#1. However, the knowledge of the Paranal ground transfer functions (simulated and later measured[6]) allows to obtain a first estimate on the impact of slewing Enclosure #1 on the other UT's. Figure 10 shows the resulting *simulated* contrast loss. While the impact for infrared observations appears acceptable, a potential problem remains for visible observation.

It can therefore be concluded that:

- the fringe contrast loss remains below or very close to the tight error budget for all mechanisms and for enclosure rotation at all tracking speeds,
- the impact of slewing one enclosure while other telescopes observe for VLTI is a potential difficulty which remains to be assessed, especially for future observation in the visible. If this problem persists, possible remedies include further optimization of the dome rotation mechanism and co-ordination of operations at Observatory level.

3. SECONDARY MIRROR AXIAL STABILITY

A number of tests, specific to VLTI, were performed in parallel to the acceptance tests of the first secondary mirror (M2) Unit at Dornier (Germany) in November 1997. The goal was to verify the axial stability of the M2 at the nanometer level in the following cases:

- after a focusing / centering step,
- during Field Stabilization (i.e. fast tip-tilt correction of atmospheric and wind load effects),
- during Chopping for observation in the thermal IR with the MIDI[7] instrument.

Measurements were performed using the two setups developed by Dornier for the acceptance tests[8]. Figure 11 and Figure 12 show the test configuration in the spiders. The mirror displacement was measured at 3 locations on its outer edge (120° apart) by laser interferometers from Optodyne (Laser Doppler Displacement Meters -LDDM- type DBIII). The signals were then processed in Matlab to deduce not only angular information but also the axial displacement of the mirror vertex and the corresponding OPL variation.

Figure 13 shows the M2 axial displacement during a 5μm focusing step combined with a 20μm centering step simulating a typical active optics correction. The requirement set by the VLTI is that vibrations possibly excited by these actions shall be damped enough, after 3 seconds, to reach the OPL stability requirements. No excitation of eigen-modes can be seen. The resulting stability is dominated by vibrations around 25Hz which were identified as originating from the surrounding laboratory environment.

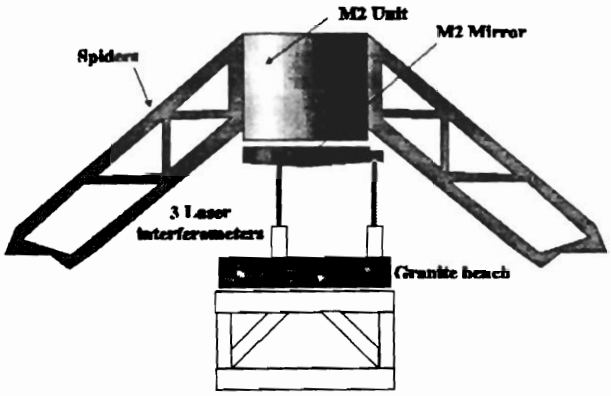

Figure 11: Test setup used to measure the axial stability performance of the M2 relevant for VLTI

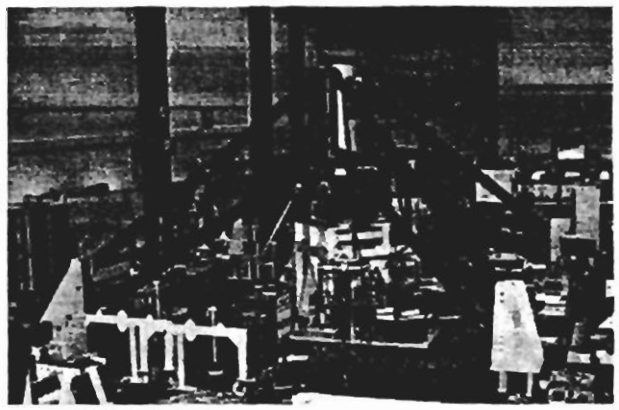

Figure 12: Picture of the M2 spider test setup at Dornier, Germany.

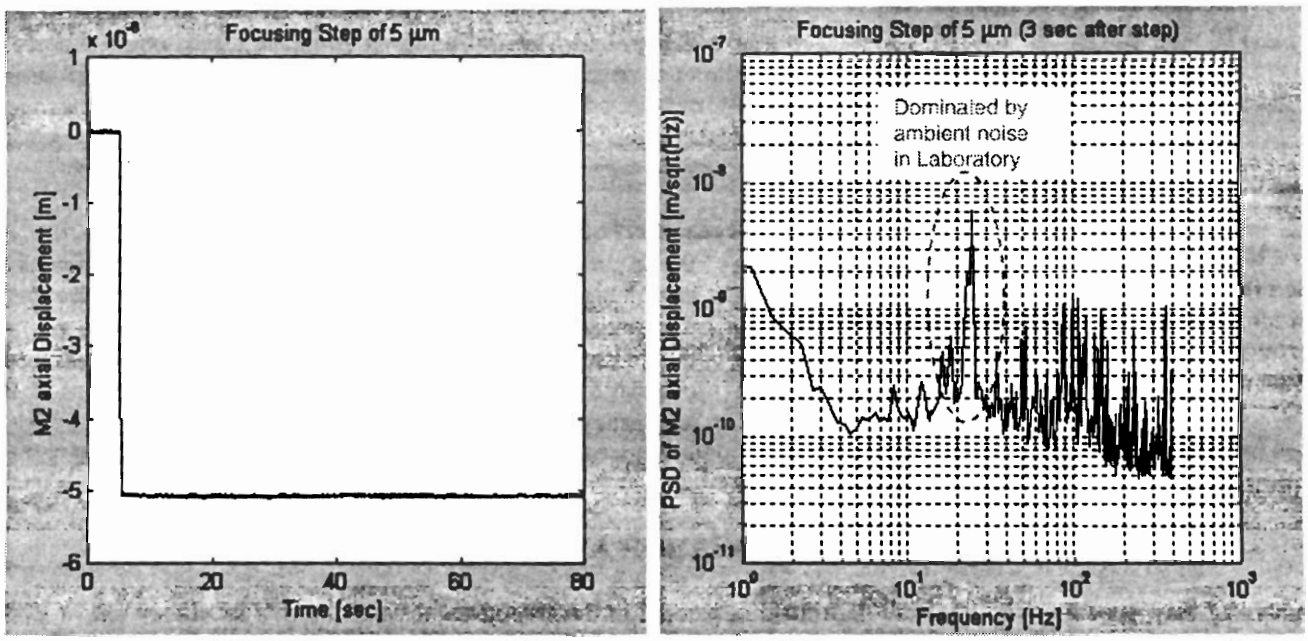

Figure 13: M2 axial stability after a 5 µm focusing step. Results: after 3 sec settling time, σ_{OPD}=9, 14, 15 nm rms over 10, 48, 290 msec (dominated by environmental noise around 25Hz).

Figure 14 shows the results during a chopping run with the following parameters: amplitude=120 arcsec (i.e. max M2 chopping throw corresponding to 30 arcsec on the sky), frequency=1Hz (typical frequency currently considered for MIDI). A cross-coupling between the tilt angle and the M2 axial position can be clearly seen. It amounts to about 0.3 µm displacement for a 120 arcsec tilt. This is explained by a 0.5 mm misalignment between the mirror's center of rotation and its vertex. This value is within the specified range. This 0.3µm displacement which corresponds to only $\lambda/16$ OPL at 10 µm is in any case not affecting the instrument since the "off" position is used to measure the sky background where no fringe pattern is observed. More relevant is the repeatability of the "on" position which can be deduced from the long-term accuracy of the tilt positions during chopping runs. This has been measured to be below the required 0.3 arcsec requirement[8]. The corresponding OPL due to cross-coupling is in the nanometer range!

For what concerns the dynamic errors, the spectrum of OPL fluctuations was computed on each plateau (after the specified 20msec dead-time allowed for settling) and averaged over several cycles. The spectrum is shown in Figure 14. The main contributor is the 100Hz axial mode of the M2 unit which was specified to be above 60 Hz. The OPL variation amounts to

183 nm rms over 290 msec exposure time, therefore within the 225 nm budget. The result shown here represents the worst case of all measurements performed which were usually around 100nm. This means that chopping can be used for the MIDI instrument without a significant impact on the measured contrast.

The time series obtained during chopping runs were then used to compute the transfer function OPD/M2 tilt shown on Figure 15. This transfer function was used to compute the induced OPD when correcting, in Field Stabilization mode, the atmospheric tilt. The multiplication of this transfer function squared by the PSD of the atmospheric tilt enables to compute the PSD of the induced OPD shown on Figure 15. The resulting OPD fluctuations are below 1 nm rms for all observing wavelengths. A similar computation was done for correction of residual tracking errors due to wind load on the telescope tube and the results on OPL fluctuation are even lower. This demonstrates that the M2 axial stability is fully adequate to perform Field Stabilization correction during interferometric observation, although it was originally planned to use a smaller dedicated steering mirror (M8) in the coudé train. The consequences are savings in development cost and improvement of thermal infrared performance (the beam wanders on M1 only).

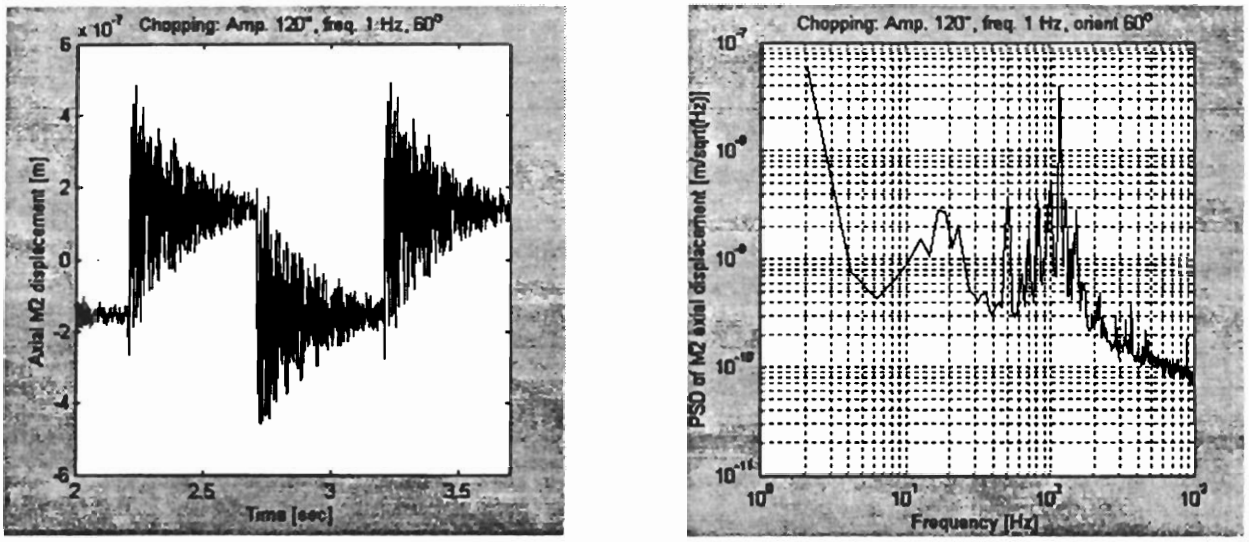

Figure 14: M2 axial stability during chopping. Results: on each plateau after 20 msec settling time, σ_{OPD}=183 nm rms over 290 msec (spec=225 nm)

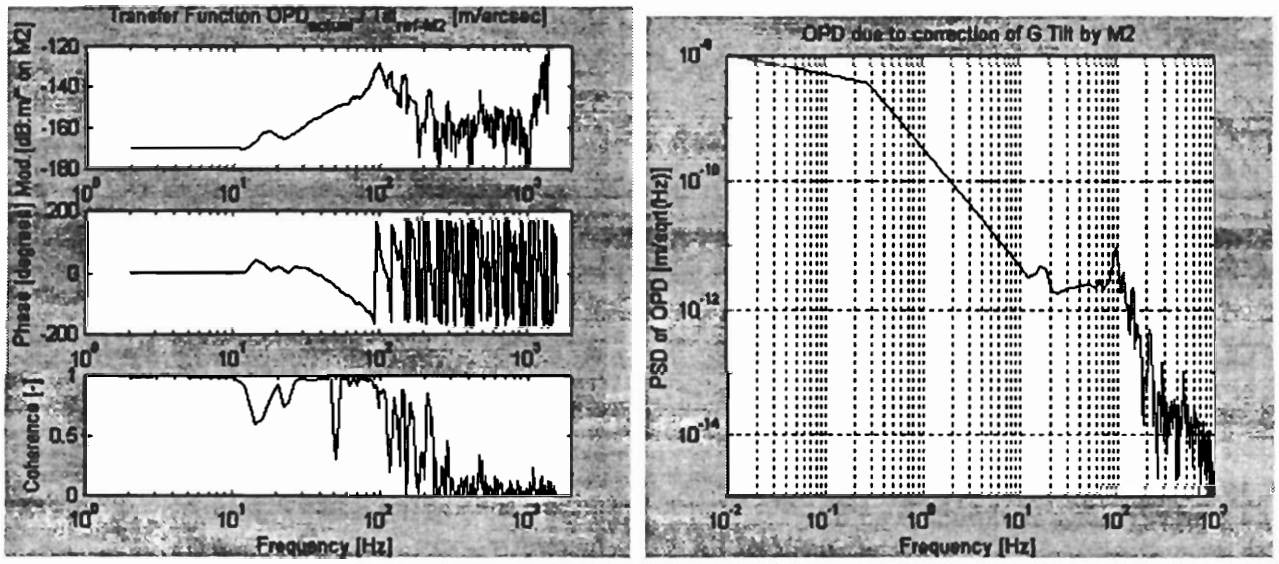

Figure 15: M2 axial stability during Field Stabilization (correction of atmospheric G-tilt). Results: σOPD due to M2 linear response <1 nm rms over 10, 48, or 290 msec , i.e. for all observing wavelengths

4. TELESCOPE STRUCTURE STABILITY

First direct measurements of the vibration level on the partially-integrated UT Main Structure were performed at Paranal in January 1998. Although the UT#1 was still equipped with dummy mirrors and mirror supports, it was the first opportunity to obtain information concerning the effects of various vibration sources which could not be assessed before and were still major unknown.

The goal was to determine vibration levels on the structure itself due to the following vibration sources:

- Hydrostatic Bearing System (HBS) noise,
- Electronics and Liquid Cooling System noise
- Motors and axes control noise at various tracking speeds

The setup is shown on Figure 16. Accelerometers were placed directly on the structure at the following locations:

- the M1 dummy,
- the M2 dummy,
- the dummy M3 tower,
- the Nasmyth adaptor flange (close to the future M4 location),
- the attachment flanges of the coudé mirror M5
- the attachment flanges of the coudé mirror M6.

Pictures of the accelerometers mounted on the dummy M2 and on the dummy M3 tower can be seen on Figure 17 and Figure 22.

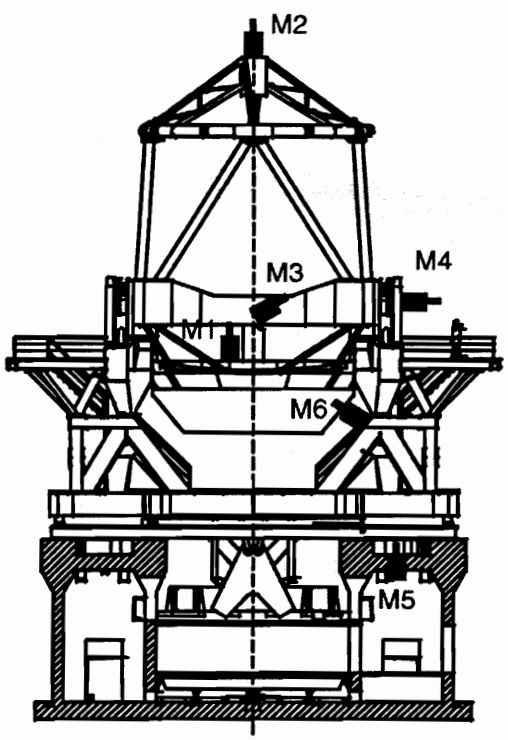

Figure 16: Accelerometer locations for the first direct measurement of vibrations on the UT#1.

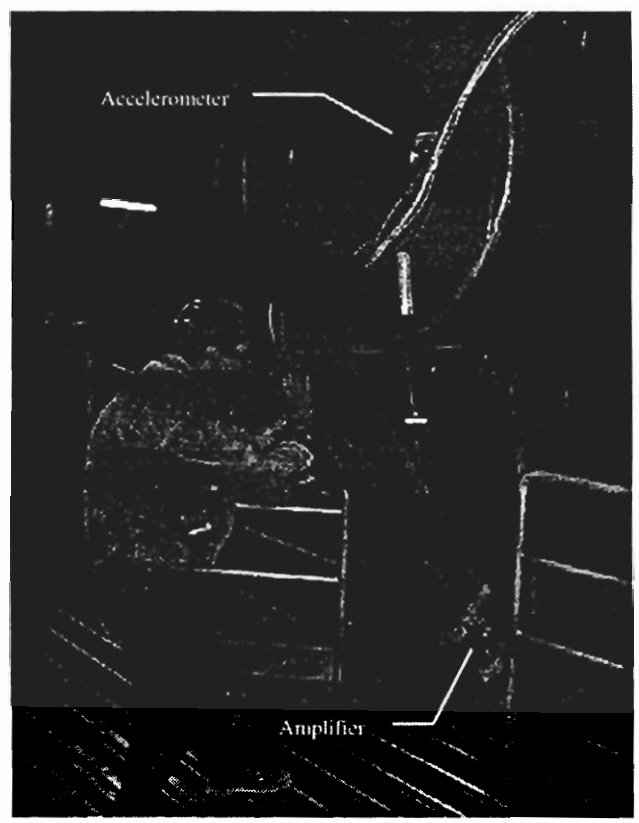

Figure 17: Accelerometer mounted on the M2 dummy

The following measurement hardware was used:

- 4 low-noise Wilcoxon Accelerometers 731A
- 2 Sunstrand QA2000 accelerometers
- 2 DSPT SigLab acquisition units + PC running Matlab

The six acceleration signals were recorded during about 30 seconds (see Figure 18) and were later linearly combined with the proper coefficients to derive the corresponding OPL fluctuation at the telescope output and to compute the associated visibility loss. All measurements were done at night after the construction activities had stopped.

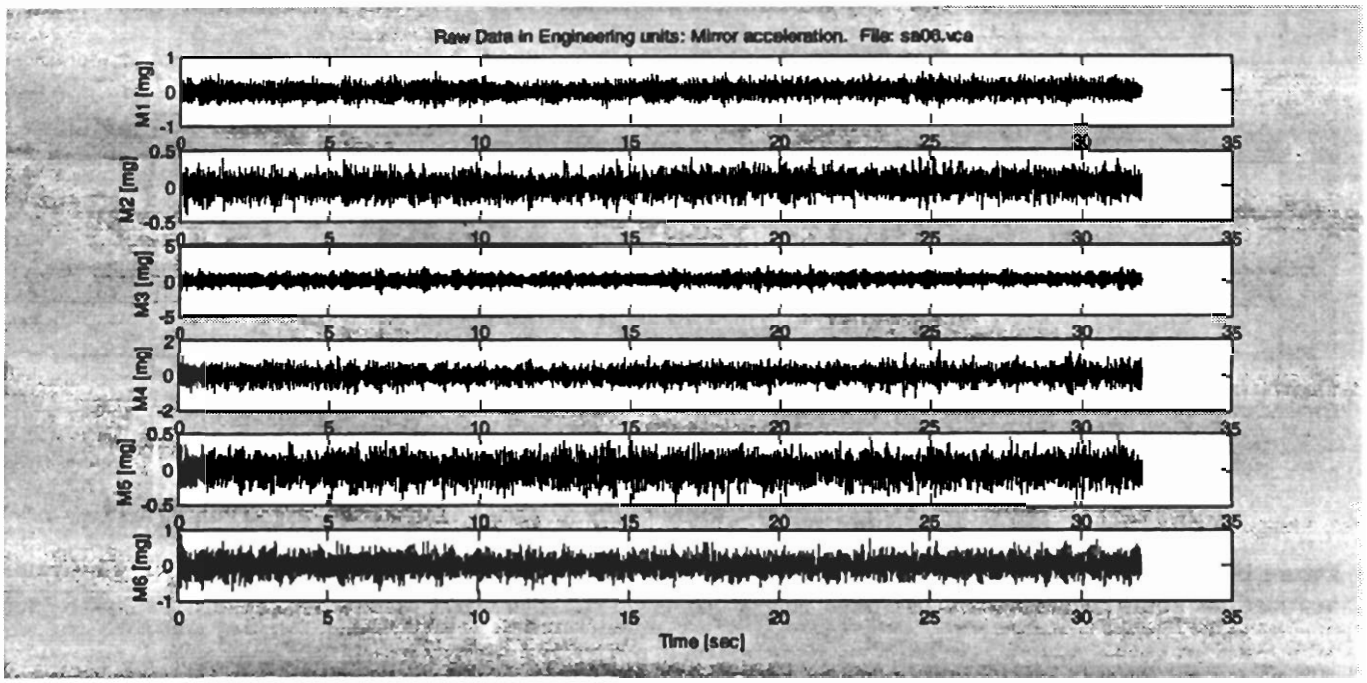

Figure 18: Example of signals recorded by the accelerometers located on the UT structure during tracking at 150"/sec Azimuth speed.

Figure 19 and Figure 20 summarize the visibility loss induced by the various perturbation sources. The loss is shown for observations at 0.6µm (upper), 2.2µm (middle) and 10µm (lower). The contribution from each mirror is plotted along the x-axis as well as the total visibility loss obtained from the linear combination.

The left-most graph of Figure 19 shows the background noise with all equipment switched off except the temporary diesel generator used to provide electrical power (see also section 2). The middle graph shows the effect of switching on the Hydrostatic Bearing System. This result is particularly important because it indicates that this most unknown and critical vibration source remains at an acceptable level even though slightly above the specification for visible observation. It is believed that improvement will occur in the future. Indeed, at the time of the measurements, some air was apparently still trapped in the hydraulic circuit creating audible noise in the supply pipes.
The effect of the liquid cooling circuit is shown on the right graph. It indicates good performance for infrared wavelength. However, the disturbance is still too high for observations in the visible. It is dominated by the contribution of the M2 whose exact origin is not clear. Improvement can also be expected with the final cooling system. This system will use heat exchangers located some 100m away from the telescopes while the temporary cooling system tested here used relatively noisy fans located just outside the enclosure.

Concerning the impact of telescope tracking, only a preliminary characterization could be performed. Indeed, the position encoders were not yet operational at that time. Therefore, the telescope was moved in velocity mode using the tachometer signal and, more important, the commutation of the motor phases was still done using the much less accurate built-in Hall Sensors. Consequently, important disturbances were created by the motors resulting in clearly audible background noise and

shocks. These preliminary results can be seen in Figure 20. Except for the thermal infrared, disturbance levels are clearly too high. However, it is expected that these results will drastically improve in the final operational configuration when the motor commutation will be done using the high-accuracy Heidenhain position encoders. Also, the results were dominated by the response of the M3 accelerometer. A closer look at the spectrum of this accelerometer (see Figure 21) evidenced the presence of high-amplitude eigen-modes around 50 and 200Hz originating from the dummy M3 tower and the accelerometer support bracket (see Figure 22). This dominating vibration is evidently not representative of the final configuration with the real M3 tower and should disappear.

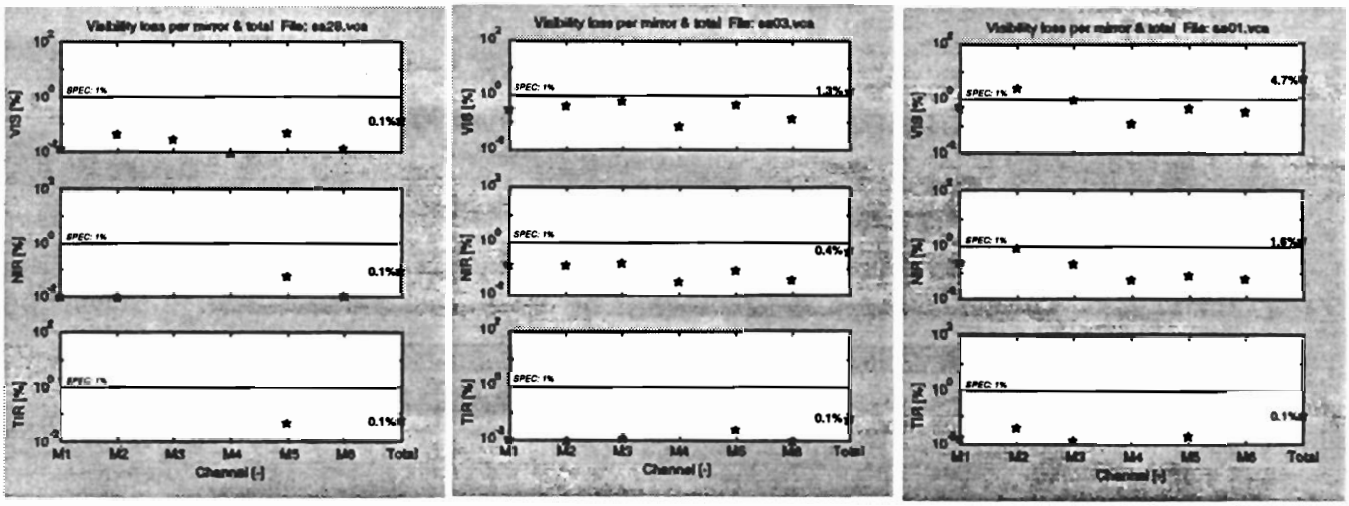

All OFF Hydraulics ON Hydraulics + Cooling ON

Figure 19: Visibility loss inside UT from first direct acceleration measurements on the structure. Effect of hydraulic bearings and liquid cooling system.

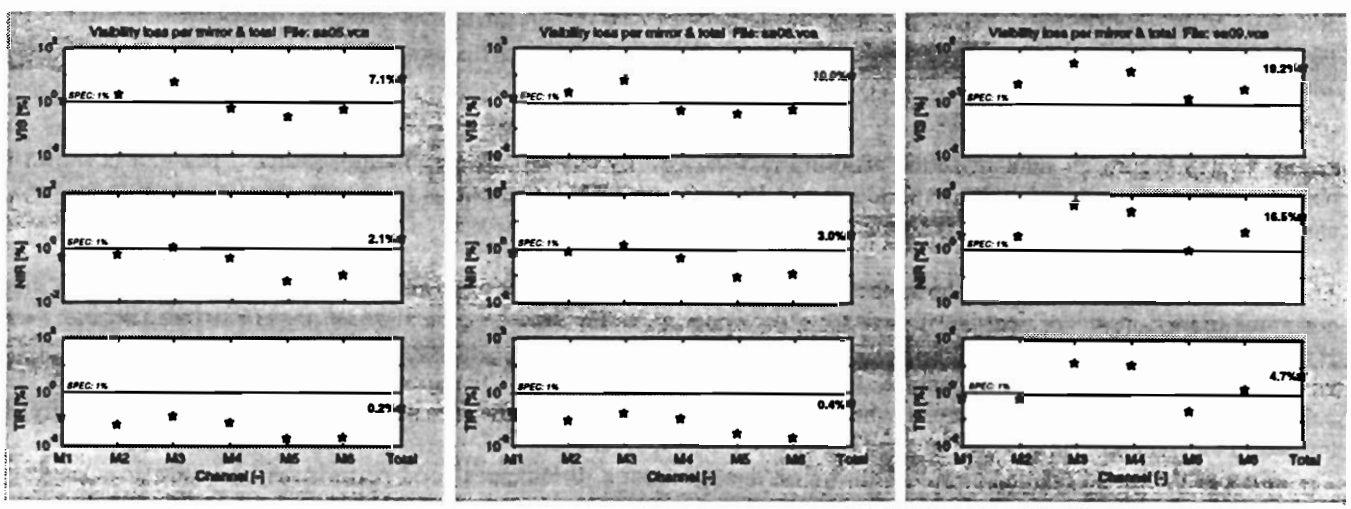

Motor ON (zero tracking speed) Tracking at Az:150"/sec Tracking at 1500"/sec (max)

Figure 20: Visibility loss inside UT from first direct acceleration measurements on the structure. Preliminary assessment of the effect of motors during tracking. The fact that the motor commutation was still done using the Hall sensors instead of the high-accuracy position encoders together with the fact that the results are dominated by non-representative eigen-modes of the M3 accelerometer mounting gives confidence that better results will be obtained in the fully integrated telescope in operational configuration to be measured soon.

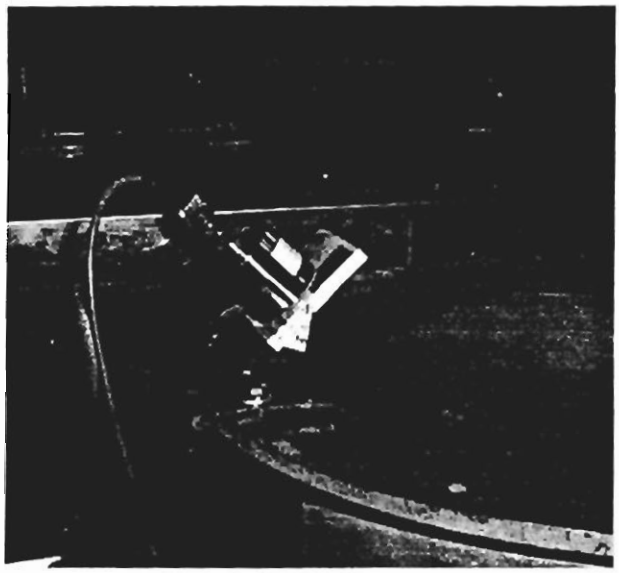

Figure 22: Accelerometer mounting on the dummy M3 tower

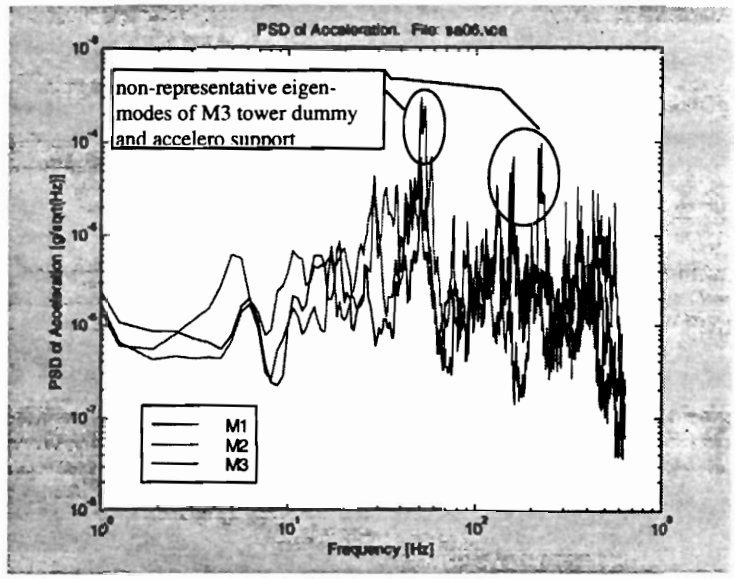

Figure 21: Example of acceleration PSD measured at M1, M2 and M3 locations during tracking

5. CONCLUSION

We have presented first OPL stability results derived from measurements performed on some VLT subsystems. The achieved performance are generally very good. Some critical issues for which we had no answer yet successfully passed the test. This includes the vibrations generated by the enclosure during tracking, the M2 axial stability after a focus step or during chopping and field stabilization, and the noise of the hydrostatic bearing system. On the other hand, some disturbance sources have shown contrast loss in excess of the 1% requirement. This includes the vibrations affecting one telescope while the enclosure of an other telescope is slewing and the OPL stability during telescope tracking. In these cases, however, future improvement are very likely to occur in the final operational telescope configuration. These items will be further addressed during commissioning test on the UT#1, later this summer.

6. ACKNOWLEDGMENTS

We wish to thank those colleagues who helped in performing these measurements, in particular G. Jander (M2), S. Lévêque (Enclosure), M. Quattri and T. Erm (Main Structure).

7. REFERENCES

1. J.M. Mariotti et al., "The VLTI Program: a status report", *in these Proceedings.*
2. B. Koehler, "Factors affecting the performance of stellar interferometers; application to the VLTI Error Budgets", *NATO ASI Series, High Angular Resolution in Astrophysics, Kluwer, Les Houches, Winter school* (April 1996).
3. B. Koehler et al., "Engineering aspects of environmental factors in VLTI," in *J. Breckinridge (ed.), Amplitude and Intensity Spatial Interferometry II*, SPIE Proceedings **Vol. 2200** (1994).
4. B. Koehler et al., "Results of studies on the environmental factors affecting the VLTI performance" in *Proc. SPIE conference, Optical Telescopes of Today and Tomorrow, Landskrona*, SPIE Proceedings **Vol. 2871** (May 1996), pp544-555.
5. B. Koehler, "Very Large Telescope Interferometer: Chasing the nanometric vibrations on 8-meter telescopes" in *Proc. of Space Micro-dynamics and Accurate Control Symposium (SMACS2), CNES, Toulouse*, (May 1997), pp165-178.
6. B. Koehler, "Hunting the bad vibes at Paranal" in ESO's *The Messenger*, **N° 76**, June 1994.
7. C. Leinert et al., "MIDI: the mid-infrared interferometric instrument for the VLTI", in *these Proceedings.*
8. R. Barho et al. "VLT Secondary Mirror Unit Performance and Test Results", in *these Proceedings.*